Proceedings of the IASS 2024 Symposium
Redefining the Art of Structural Design
August 26-30, 2024, Zurich, Switzerland
Philippe Block, Giulia Boller, Catherine DeWolf,
Jacqueline Pauli, Walter Kaufmann (eds.)

Minimal surface based elastic gridshell design

Xinye LI[*a,b], Mohammad MANSOURI[e], Ahmed ELSHAFEI[c,d]

[*a] Dept. of Structural Engineering, College of Civil Engineering,Tongji University
No.1239, Si Ping Rood, Shanghai 200092, P.R. China
Xinyeli@tongji.edu.cn

[b] Institute of Discrete Mathematics and Geometry, TU Wien, Vienna, Austria
[c] Laboratoire GSA, ENSA Paris Malaquais, Université PSL, Paris, France
[d] CMAT - Centro de Matemática, Universidade do Minho, Campus de Gualtar, Portugal
[e] Laboratoire LACTH, ENSAP Lille, Université de Lille, Villeneuve d'Ascq, France

Abstract

In this research, we present and elaborate on a geometrical morphogenetic approach for generating minimal surface patches (MS-patches) tailored for elastic gridshell design and fabrication. We highlight the essential role of assessing pre-stress levels through geometrical analysis, noting their direct impact on assembly challenges. Additionally, we pay close attention to both structural performance and architectural functionality. Our approach utilizes analytical techniques to generate *conformal iso-conjugate* MS-patches from a conformal spherical image induced by a holomorphic map, which also ensures the correspondence between the induced principal and asymptotic networks. These geometric constructions are then converted into morphological design tools, opening up a design space ripe for exploration. Assembling difficulty is analyzed by checking the curvature of principal strips and torsion angle of asymptotic curves, alongside structural performance is checked by global deflection under self-weight. Architectural functionality is assessed through the ratio between usable area and covered area. This approach aims at bridging form and function, showing the rich design space within the realm of minimal surfaces.

Keywords: Minimal Surface, Elastic Gridshell, Holomorphic Functions, Principal Networks, Asymptotic Networks, Differential Geometry, Pre-stress Level, Architectural Fabrication.

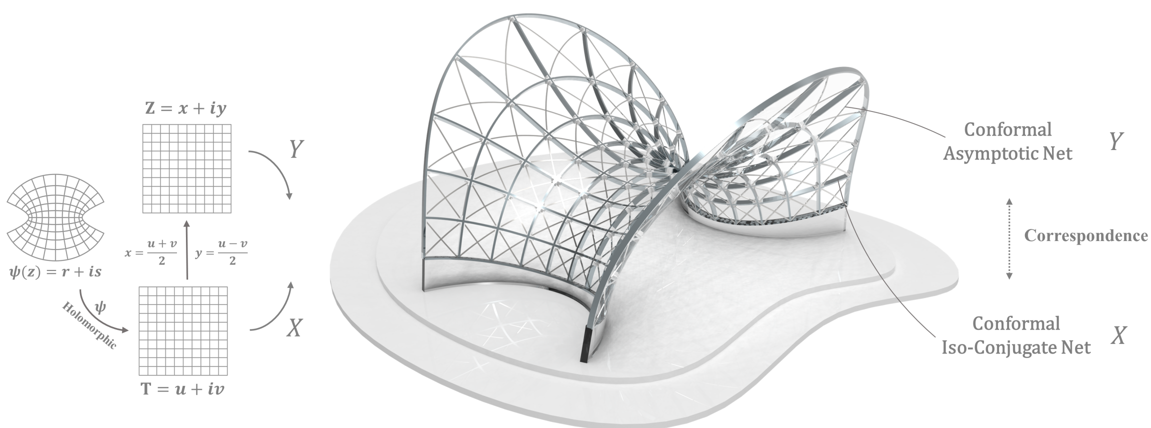

Figure 1: Corresponding principal-asymptotic networks on a MS-patch from a holomorphic function.

1. Introduction

Most of the time, freeform structure design is not regarded as an eco-friendly design strategy, due to the complexity of the design. First, the manufacturing process of elements is time-consuming and expensive; Second, the construction process is labour intensive and involves high-tech tricks for assembly. In light of this issue, we consider whether it is possible to design freeform surface structures using standardized, easily constructed structural components and a simple assembling process while ensuring the freedom of surface forms and their structural performance. This topic is highly related to geometry, and the field of architectural geometry (Helmut Pottmann et al.[1]) emerged precisely as a response to this challenge, aiming at sustainable fabrication methods for freeform structures. Here we focus on the classic surface: minimal surface (MS), aiming at designing a complex supporting grid system with highly efficient in manufacturing by simplifying the assembling process and facilitating the construction process.

1.1. Previous work on laths generated from special curves on surfaces

Based on their geometric characteristics, we recall some special surfaces and special curves on the surface. Classical examples of such rational special surfaces are: minimal surfaces, constant Gaussian curvature surfaces, constant mean curvature surfaces, or more generally Weingarten surfaces. Beneficial curves on surfaces include: principal curves, asymptotic curves, (pseudo-)geodesic curves, among others. In gridshell design, the lath stands as the primary component, necessitating a heightened focus on the curves part. Among these advantageous curves, laths generated from geodesic curves exhibit reduced out-of-plane stiffness and are prone to out of plane buckling under external loads, making them unsuitable for standalone use in large-scale constructions (S. Pillwein et al.[2]). Conversely, gridshells generated from pseudo-geodesic curves provide superior in-plane and out-of-plane stiffness; however, they are challenged by complex joints and a restricted range of potential freeform shapes (B. Wang et al. [3], R. Mesnil et al.[4]). Gridshells generated from asymptotic curves hold the benefit of strips that approximate straight lines once unfolded (albeit with some distortion) (D. Pellis et al.[5], E. Schling et al. [6]) (shown as Figure 2(e)). Yet, assembling these asymptotic strips into the desired shape necessitates both pre-twisting and pre-bending along two axes, inducing certain levels of pre-stress adverseness to the assembly process. Gridshell designs employing principal curves afford the advantage of right angled joints (Figure 2(a)) and planer panels (Figure 2(b)), also the surface normal strips generated from principal curvature lines are developable that can be easily unrolled (without distortion) into a planar state (Figure 2(d)). Similar work can be found from E. Schling et al. [7] and Wedl, Marilies[8].

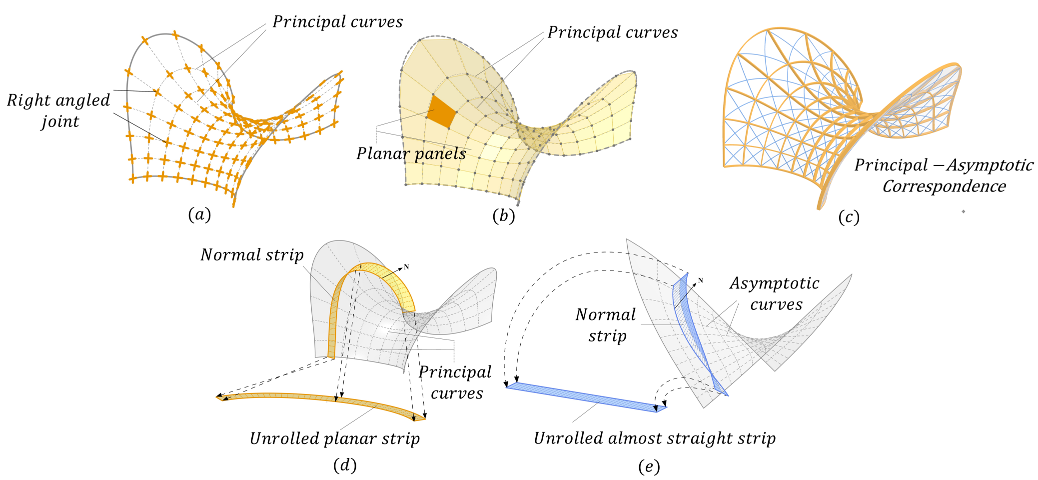

Figure 2: Geometric properties of MS-patches corresponding to fabrication advantages.

2. Geometry

As mentioned in the introduction our focus is constructing curve networks on MS to be the basis of gridshell design. Recalling the properties of special curves on surfaces discussed in the Introduction, we focus on principal and asymptotic curves on MS. There are primarily two approaches to constructing minimal surfaces: precise modeling methods and approximation modeling methods. The precise modeling methods can be categorized into two main types: the representation and construction of control meshes for certain special minimal surfaces, and the exploration and properties of isothermal parameterized minimal surfaces. The approximation modeling methods can be classified into three main types: numerical approximation methods, approximation methods based on linear partial differential equations, and approximation methods based on energy function optimization.
Unlike the approach discussed in the introduction (D. Pellis et al.[5], E. Schling et al. [6]), which utilizes approximation methods to construct minimal surfaces and identify asymptotic and principal curvature lines on minimal surfaces, here we adopt precise modeling methods, starting from mathematical definitions, to construct minimal surfaces with isothermal parameters and explore a broader modeling space. For this, we will give the construction of conformal iso-conjugate MS-patches, for more details see (L. Eisenhart [9]) and (U. Dierkes et al. [10]).

2.1. Construction of conformal iso-conjugate MS-patches

Based on classical works from differential geometry (L. Eisenhart [9]), here we construct a method for generating what we will call conformal iso-conjugate MS-patches. To begin, we recall some of the basic necessary geometric notions. In the context of this paper, a surface in $\mathbb{R}^3$ equipped with its standard scalar product, is always given by a smooth parametric patch $X(u,v)$ with the coordinates (u,v) defined on an open subset of $\mathbb{R}^2$. The partial derivatives of the patch are denoted by X_u, X_v and its normal vector field denoted by N. Note that the normal is also seen as a smooth patch $N(u,v)$ on the unit sphere $\mathbb{S}^2$ and referred to as the spherical image of the patch X. Using the vector fields X_u, X_v, N we determine the coefficients E, F, G, e, f, g of the first and second fundamental form, in addition to the Gaussian curvature $\mathcal{K}$ and Mean curvature $\mathcal{H}$. Recall that the Gaussian curvature $\mathcal{K}$ is given as the product of the two principal curvatures k_1, k_2 and the Mean curvature $\mathcal{H}$ as their average, and are given by (Equation (1)). Next, note that when the coefficients F and f are equal to zero, the patch X is said to be a principal patch (i.e. its coordinate lines are lines of curvatures). Similarly, when the coefficients e and g are equal to zero, the patch X is said to be an asymptotic patch (i.e. its coordinate lines are asymptotic lines). Finally, a conformal iso-conjugate MS-patch X is characterized by having the Mean curvature $\mathcal{H}$ vanishing identically and its fundamental coefficients satisfying the conditions in Equation (2).

$$\mathcal{K} = \frac{eg - f^2}{EG - F^2} \quad , \quad \mathcal{H} = \frac{eG - 2fF + gE}{EG - F^2} \tag{1}$$

$$F = 0 \ , \ E = G \ \text{(Conformal)} \quad , \quad f = 0 \ , \ e = -g \ \text{(Iso-conjugate)} \tag{2}$$

It turns out that these two properties are connected for MS-patches, this is due to a classical theorem from (L. Eisenhart [9]) these two properties are connected for MS-patches. More precisely, the theorem states that if X is a conformal patch then, its N is conformal if and only if X is MS-patch. Moreover, such a conformal MS-patch X necessarily satisfies $e = -g$. From a fabrication point of view these properties are quite advantageous. In more accurate terms, since the conformal property is in particular orthogonal resulting in the characteristic of preserving right angles on the network, (Figure 2(a)). On the other hand, since the iso-conjugate property is in particular conjugate, it facilitates the construction of planar panels (Figure 2(b)). Let us explain the geometric construction of the conformal iso-conjugate MS-patch X. The idea is to start by a conformal patch N on $\mathbb{S}^2$ then determine a conformal iso-conjugate MS-patch

X (for which N is normal) by solving a first order partial differential system (L. Eisenhart [9]). Now given such a conformal patch N, by conformality we have that is E and G are equal and thus denoted by $\tilde{\Lambda}$. Next, the differential system to solved (by quadratures) yield our conformal iso-conjugate MS-patch X, and is thus given by the two equations:

$$X_u = -\frac{N_u}{\tilde{\Lambda}} \;\; , \;\; X_v = \frac{N_v}{\tilde{\Lambda}}. \tag{3}$$

The next part of the construction is to generate the conformal patch N on $\mathbb{S}^2$ as a composition of the inverse of the stereographic projection N_o given by (Equation (7)) and a holomorphic map Ψ (on some domain in $\mathbb{C} \simeq \mathbb{R}^2$). This allows us to create MS-patches X corresponding to holomorphic maps Ψ.

2.2. Construction of corresponding Principal-Asymptotic networks

It is clear that our conformal iso-conjugate MS-patch $X(u, v)$ is in particular a principal patch (since it is orthogonal and conjugate). Furthermore, the fact that $X(u, v)$ is conformal and iso-conjugate comes with the extra benefit of having the corresponding "diagonal" reparameterization $Y(x, y)$ given by (Equation (4)), being conformal asymptotic. In more accurate terms, if we consider the simple change of coordinates given by the transformation:

$$\Phi(u, v) = \left(\frac{u+v}{2}, \frac{u-v}{2}\right) \qquad \text{with inverse} \qquad \zeta(x, y) = (x + y, x - y) \tag{4}$$

we obtain new parameterization $Y = X \circ \zeta$ for the minimal surface, expressed as:

$$Y(x, y) = X(x + y, x - y). \tag{5}$$

This principal MS-patch $X(u, v)$ and the asymptotic MS-patch $Y(x, y)$ naturally give rise to networks of principal, respectively asymptotic curves. By selecting a discrete number of (u, v)-curves and (x, y)-curves, each equally spaced (along the two parameters) in their respective parameter spaces, the induced principal and asymptotic networks will correspond. That is their intersection points will perfectly match with each other as seen in Figure 1

To end this section, we recall that we can choose any holomorphic function $\Psi(T)$ with $T = u + iv$ defined on some open domain in $\mathbb{C} \simeq \mathbb{R}^2$ for example:

$$\Psi(T) = T \;\; , \;\; \Psi(T) = \frac{aT + b}{cT + d} \;\; , \;\; \Psi(T) = (a + ib)T^2 \;\; , \;\; \Psi(T) = a\sin(bT + c) \;\; , \;\; \cdots \tag{6}$$

where $a, b, ...$ are real constants, introducing parameteric variation in the type. Next, we compose Ψ with the inverse of the stereographic projection N_o (from north pole) given by the expression

$$N_o = \left(\frac{2u}{u^2 + v^2 + 1}, \frac{2v}{u^2 + v^2 + 1}, \frac{u^2 + v^2 - 1}{u^2 + v^2 + 1}\right) \tag{7}$$

to obtain the conformal patch $N = N_o \circ \Psi$ which in turn is put in Equation (3). Then solving the system yields the conformal iso-conjugate MS-patch $X(u, v)$ associated to the holomorphic function Ψ.

3. Morphology

In the previous section, we provided the geometric constructions required for the generation of conformal iso-conjugate MS-patches. In this section, we use these geometric constructions construct a space of morphological exploration that we refer to as the *Space of Variants*. Furthemore, we guide the selection of variant by the following criteria: Assembly difficulty - Criterion 1, Structural performance - Criterion 2, and Architectural functionality - Criterion 3. The aim is to allow designers to observe the evaluation indicators—criteria 1,2,3 —in real- time while designing forms, optimizing the design.

3.1. Space of Variants

Our variable space includes: the selection of holomorphic functions, the choice of parameters within holomorphic functions, symmetrical reflections, and periodic transformations. For the sake of clarity and good illustration of the method, we will fix one choice of holomorphic function Ψ and use the MS-patches X arising from it as the basis surface patches used for the morphological exploration. To this end, let us then fix the choice of holomorphic function Ψ to be of **Sinus-type**, that is:

$$\Psi(T) = a\sin(bT + c) \quad , \quad T = u + iv \in \mathbb{C}\ ,\ a, b, c \in \mathbb{R} \tag{8}$$

giving rise to a conformal patch (on $\mathbb{S}^2$) defined by $N = (\Psi \circ N_o)$ given explicitly by:

$$\left(\frac{4a\cosh(bv)\sin(c+bu)}{2-a^2\cos(2(c+bu))+a^2\cosh(2bv)}, \frac{4a\sinh(bv)\cos(c+bu)}{2-a^2\cos(2(c+bu))+a^2\cosh(2bv)}, \frac{-2-a^2\cos(2(c+bu))+a^2\cosh(2bv)}{2-a^2\cos(2(c+bu))+a^2\cosh(2bv)}\right) \tag{9}$$

which upon substitution in (Equation (3)) and solving (by quadratures) yields the conformal iso-conjugate MS-patch $X(u, v)$ given explicitly by the expression:

$$\begin{pmatrix} \left(\frac{1-a^2}{4ab^2}\right)\log\left(2(\cosh(bv) - \sin(c+bu))\right) - \left(\frac{1-a^2}{4ab^2}\right)\log\left(2(\cosh(bv) + \sin(c+bu))\right) - \left(\frac{a}{2b^2}\right)\cosh(bv)\sin(c+bu) \\ \left(\frac{1+a^2}{2ab^2}\right)\arctan\left(\frac{\sinh(bv)}{\cos(c+bu)}\right) - \left(\frac{a}{2b^2}\right)\sinh(bv)\cos(c+bu) \\ \left(\frac{1}{2b^2}\right)\log\left(\cos(2(c+bu)) + \cosh(2bv)\right) \end{pmatrix} \tag{10}$$

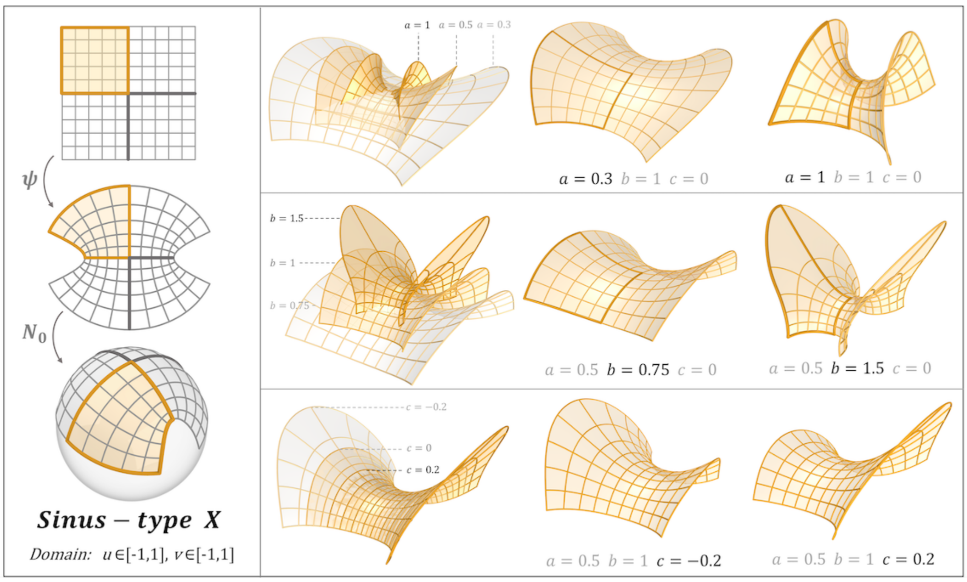

Figure 3: Variation of (Sinus-type) MS-patches X obtained from varying a, b, c.

3.2. Selection of variants

3.2.1. Assembly difficulty - Criterion 1

If we look into detail, the assembly difficulty has a clear relation to the curvature of the "normal" strips, i.e. ruled strips obtained by sweeping the normal to the surface along coordinate curves. The difficulty of assembly lies in the need to bend or twist the lath from a flat state into a predetermined shape and fix it in the specified position. These pre-bending and pre-twisting operations contribute to the so-called pre-stress level. The higher the curvature and torsion, the higher the bending stresses and shearing stresses. Now, in the Introduction, it was shown in Figure 2 (d) that every normal principal strip, i.e. the ruled u-strips (resp. v-strips) obtained by sweeping the normal N along principal u-curve $X(u, v_o)$ (resp. v-curve $X(u_o, v)$) for any fixed v_o (resp. u_o) given by:

$$\mathcal{U}(u, w) = X(u, v_o) + wN(u, v_o) \quad , \quad \text{resp. } \mathcal{V}(v, w) = X(u_o, v) + wN(u_o, v) \tag{11}$$

is developable (i.e. with zero Gaussian curvature). Since both $\mathcal{U}$ and $\mathcal{V}$ are analogous, let us consider the u-strip $\mathcal{U}$. Being developable, it follows that, such a strip does not require pre-twisting, and in certain cases where it is planar, it does not require pre-bending either. Due to developability, one of the principal curvatures of $\mathcal{U}(u, w)$ (say k_2) whose principal direction aligns with the ruling direction N is zero. It then follows that, the pre-stress level on the strip is fully contributed by the other principal curvature k_1, as seen in Figure 4. Now recalling that computation of the principal curvatures are given by the roots $\mathcal{H} \pm \sqrt{\mathcal{H}^2 - \mathcal{K}}$ and that $\mathcal{K}(\mathcal{U}) = 0$ yields that, the pre-bending curvature in the u-strip $\mathcal{U}(u, w)$ at any (u, w) is given by:

$$k_1(u, w) = 2\mathcal{H}(\mathcal{U})(u, w). \tag{12}$$

On the other hand, every normal asymptotic strips, i.e. the ruled strip obtained by sweeping the normal N along the asymptotic x-curve $Y(x, y_o)$ (resp. y-curve $Y(x_o, y)$) for any fixed y_o (resp. x_o) given by:

$$\mathcal{X}(x, t) = Y(x, y_o) + tN(x, y_o) \quad , \quad \text{resp. } \mathcal{Y}(y, t) = Y(x_o, y) + tN(x_o, y) \tag{13}$$

has the advantage of being unrolled to an almost straight band, as seen in Figure 2 (e). Since both $\mathcal{X}$ and $\mathcal{Y}$ are analogous let us consider the x-strip $\mathcal{X}$. Being non-developable (i.e. $\mathcal{K}(\mathcal{X}) \neq 0$) means that, such a strip will require a certain amount of both pre-twisting and pre-bending to take the desired shape. Here, we are more concerned with the shearing forces caused by the pre-twisting. More intuitively, the amount the ruling direction given by N rotates about the tangent to the curve $c(x) = \mathcal{X}(x, 0) = Y(x, y_o)$. Now since the curve $c(x)$ is an asymptotic curve, its normal curvature vanishes identically which means that the binormal in the Frenet frame aligns with the normal N in the Darboux frame. From another side, we recall that torsion angle $\theta(c)(x)$ of the curve $c(x)$ (seen as a spatial curve) given by:

$$\theta(c)(x) = \int_{x_0}^{x} \tau(c) \mid c' \mid dx \qquad \text{where } \tau \text{ is the torsion} \quad \tau(c) = \frac{\langle c' \times c'', c''' \rangle}{\mid c' \times c'' \mid^2} \tag{14}$$

describes the rotation of the binormal in the Frenet frame. There follows that, the rotation of N which describes the shearing stress in the x-strip $\mathcal{X}(x, t)$ can be assessed by calculating the torsion angle along the curve $c(x)$. Now, as mentioned earlier we will focus on the MS-patch of the Sinus-type with its corresponding principal-asymptotic networks arising from the patches $X(u, v)$ and $Y(x, y)$ respectively. We analyze the pre-stress levels of the two grids in question by evaluating the principal curvature k_1 and torsion angle θ, as seen in Figure 4.

This implies that once the material and its cross-section are determined, the maximum stress can be

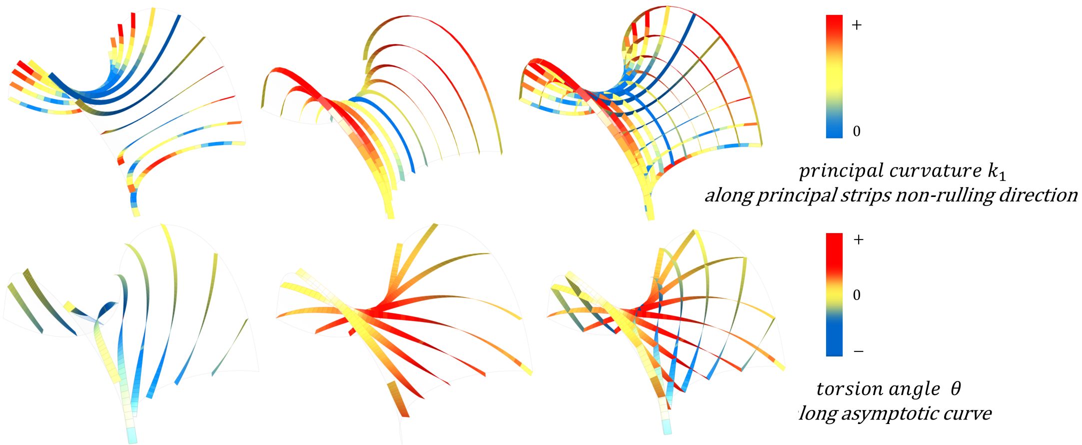

Figure 4: Top: Principal curvature k_1 of normal principal strips along principal u, v-curves on the MS-patch $X(u, v)$. Bottom: Torsion angle θ along asymptotic x, y-curves on the MS-patch $Y(x, y)$.

clearly identified. As observed, we can precisely locate the points of maximum curvature and subsequently calculate the maximum stress using formulas from the mechanics of material. Unlike the approximation method for constructing minimal surfaces, where variables may not be as easily traceable, here all parameters and their relationships are clearly defined. This allows us to accurately control the maximum stress resulting from bending or twisting and to identify the optimal solution by adjusting the parameters.

3.2.2. Structural performance - Criterion 2

Grid's stiffness is an important index for evaluating the grid's structural performance during the whole structural service period, the maximum displacement of a grid under certain load is clear to show the stiffness of the target structure. Here we test the stiffness performance under self weight while the varying parameters changes (Figure 5) using Sinus-type case for discussion (refer to section 3.1). In this study, we use Karamba3D for testing. The joints are defined as hinged, and the corner points are fixed as boundary conditions. Self-weight is applied as the load case. The model spans approximately 10 meters, with the same cross-section along the curve.

The results show that, under the same cross-section and the same load case, the order of structural stiffness is: principal + asymptotic lath > asymptotic lath > principal lath.The principal + asymptotic lath performs best is obvious, but the comparison between principal lath and asymptotic lath worth to

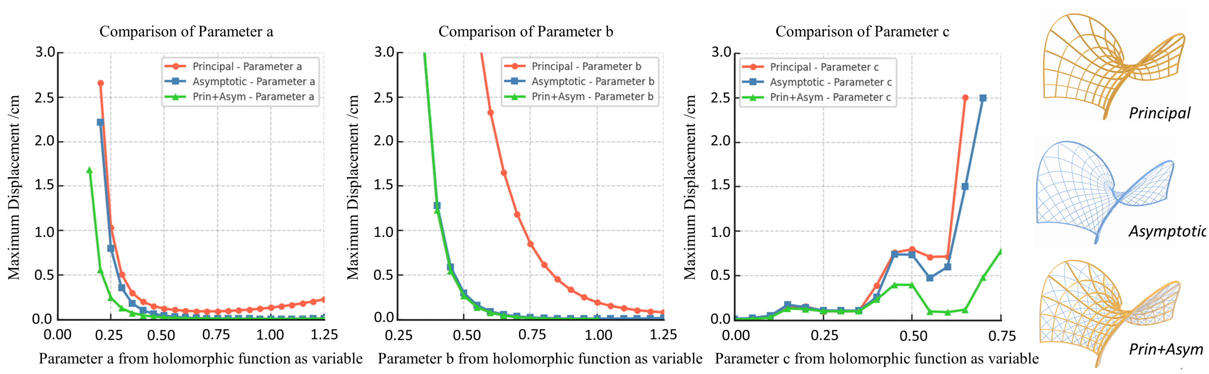

Figure 5: Maximum displacement of principal laths, asymptotic laths, and principal + asymptotic lath with sme cross-section under self weight.

have further investigation. As we found, the asymptotic curve direction aligns well with principal stress direction on minimal surface under vertical self weight in this case. Due to the page limit, we won't go to too many details. Through parametric analysis, we found that when using sinus-type as holomorphic function and considering the mechanical behavior of the structure under self-weight, the optimal range for parameter a is [0.4, 1], for parameter b is greater than 0.6, and for parameter c is [0, 0.3].

3.2.3. Architectural functionality - Criterion 3

Architectural functionality can be represented by the volume $\mathcal{V}_{usable}$ of the region on the ground under the surface, whose points have a vertical distance to the surface greater than some constant (typically an average human height), as shown in Figure 6. Now, we define the ratio $\mathcal{R}$ to be the ratio between the usable area $\mathcal{A}_{usable}$ (can be step into) to the total covered area $\mathcal{A}_{total}$, that is

$$\mathcal{R} = \frac{\mathcal{A}_{usable}}{\mathcal{A}_{total}} \quad , \quad \text{maximal equals 1.} \tag{15}$$

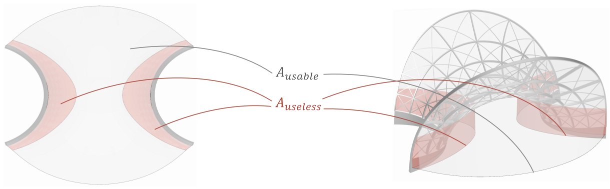

Figure 6: Green areas under the shell indicate usable volume, as opposed to the red areas.

By comparing the spatiality-ratios of different variants (as the parameters vary), designers can gain insights into which designs are more spatially efficient and better suited to the intended use and context.

4. Design cases

In this section, we present several architectural interpretations of minimal surfaces generated and constructed according to the properties and methods previously mentioned. These models were created as part of the *Morphology* course with third-year architecture students at ENSAP-Lille. Each group selected a minimal surface from the library of surfaces (with double patches) derived from various instances of the variant's space. The different considerations and interpretations, ranging from orientation and assembly to intersection, structure, and materiality, enabled the realization of diverse and rich architectural pavilions. Throughout the design process, the rationality of construction was maintained, facilitated by the properties of the principal and asymptotic double networks elaborated earlier. These design cases showcase the creative potential inherent in minimal surfaces while demonstrating the application of theoretical concepts to practical architectural projects.

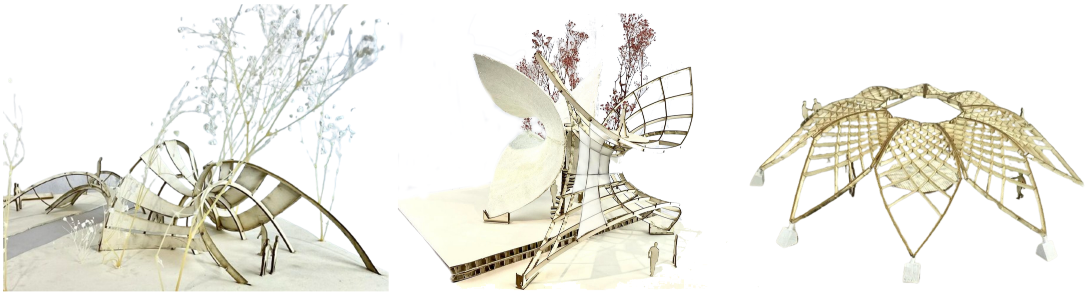

Figure 7: Several design cases made using the above proposed design approach.

5. Conclusion

In this work, we explored the construction of minimal surfaces using precise mathematical methods and considered the parametric construction of minimal surfaces based on manufacturing requirements. We developed a parameterization method for quadrilateral mesh gridshells based on the principal curvature direction and asymptotic direction. In contrast, approximation methods for constructing minimal surfaces are limited by the initial input mesh, where the initial form influences the final optimization results and cannot simultaneously accommodate other functional adjustments to the shape. Our approach, using precise mathematical methods to construct parametric surfaces, allows us to explore parameter variations to find shapes more suitable for specific construction requirements while ensuring the construction needs are met, as shown in Section 3.2.

Although approximation methods direct towards a specific target surface, designers have sufficient flexibility at the design's inception to conceptualize their design. Conversely, the explorative shape space for precisely constructed parametric minimal surfaces must be grounded in rigorous mathematical derivations. The potential forms of minimal surfaces are infinite, and no universal parametric minimal surface can encompass all possible minimal surface forms. Therefore, exploring more mathematical transformations within this method to introduce more shape-related variables will enrich the designer's available design space. Here, we introduced shape parameters through the choose of holomorphic functions. Due to page limitations, we cannot detail every possible type here. Future work can introduce more potential shape parameters and geometric transformations.

While simplifying component manufacturing complexity, design also introduces challenges in assembly. Future work needs to discuss, improve, and conduct refined finite element analysis on the existing assembly processes.

Acknowledgements

The research of the first author was supported by China Scholarship Council (CSC), and the research of the third author was partially financed by Portuguese Funds through FCT (Fundação para a Ciência e a Tecnologia) within the Projects UIDB/00013/2020 and UIDP/00013/2020.

References

[1] H. Pottmann, A. Asperl, M. Hofer, and A. Kilian, *Architectural Geometry*. Bentley Institute Press, 2007.

[2] S. Pillwein, K. Leimer, M. Birsak, and P. Musialski, "On elastic geodesic grids and their planar to spatial deployment," *ACM Trans. Graph.*, vol. 39, no. 4, 2020.

[3] B. Wang, H. Wang, E. Schling, and H. Pottmann, "Rectifying strip patterns," *ACM Trans. Graph.*, vol. 42, no. 6, 2023.

[4] R. Mesnil and O. Baverel, "Pseudo-geodesic gridshells," *Engineering Structures*, vol. 279, 2023.

[5] D. Pellis, H. Wang, M. Kilian, F. Rist, H. Pottmann, and C. Müller, "Principal symmetric meshes," *ACM Transactions on Graphics*, vol. 39, no. 4, 2020.

[6] E. Schling and Z. Wan, "A geometry-based design approach and structural behaviour for an asymptotic curtain wall system," *Journal of Building Engineering*, vol. 52, 2022.

[7] E. Schling, D. Hitrec, and R. Barthel, "Designing Grid Structures Using Asymptotic Curve Networks," in *Design Modelling Symposium Paris 2017. Humanizing Digital Reality*, Springer Singapore, 2017, pp. 125–140.

[8] M. Wedl, "Ein Beitrag zur Erstellung einer Gitterschale unter der Verwendung asymptotischer Kurven auf Minimalflächen," de, Diploma Thesis, Technische Universität Wien, 2020.

[9] L. Eisenhart, *A Treatise on Differential Geometry of Curves and Surfaces*. Boston: Ginn and Company, 1909.

[10] U. Dierkes, S. Hildebrandt, and F. Sauvigny, *Minimal surfaces*. Berlin, Heidelberg: Springer, 1992.